Fatigue monitoring of flax fibre reinforced epoxy composites using integrated fibre-optical FBG sensors

Szebényi G., Blößl Y., Hegedűs G., Tábi T., Czigány T., Schledjewski R.

# Fatigue monitoring of flax fibre reinforced epoxy composites using integrated fibre-optical FBG sensors

Gábor Szebényi [a,*], Yannick Blößl [b], Gergely Hegedüs [a], Tamás Tábi [a,c], Tibor Czigany [a,c], Ralf Schledjewski [b]

[a] Department of Polymer Engineering, Faculty of Mechanical Engineering, Budapest University of Technology and Economics, Budapest, Hungary
[b] Processing of Composites Group, Department Polymer Engineering and Science, Montanuniversität Leoben, Leoben, Austria
[c] MTA–BME Research Group for Composite Science and Technology, Budapest, Hungary

## ARTICLE INFO

## ABSTRACT

We demonstrated the applicability of integrated Fibre Bragg Grating (FBG) sensors in the case of flax fabric reinforced epoxy matrix composites produced by resin transfer moulding (RTM). FBG sensors were integrated between the reinforcing layers of the composites. We verified the robustness of FBG-based strain measurement by comparing it to strain gauge strain measurement, optical fine strain measurement and deflection measurement from crosshead displacement during four-point flexural tests. After the extensive characterization of the static properties of the composite material, fatigue tests were performed in the same setup on the specimens with integrated FBG sensors. We demonstrated that with the integrated optical fibres, the cyclic creep strain of the composites could be monitored, which could be used as a criterion to predict the fatigue failure of the composites. The proposed technique can provide an effective and robust way for periodic condition monitoring of composite structures, especially in natural fibre reinforced composites, where creep is more pronounced than in the case of synthetic fibre reinforced composites.

## 1. Introduction

### 1.1. Motivation for condition monitoring

Composites are used in numerous fields of application and therefore there is a growing interest in monitoring the condition of composite structures during their lifetime [1–3]. The simulation of the behaviour of composites is still challenging due to its complexity [4–6], thus an essential part of the investigation of long-term properties of composite structures is empirical investigation. Various techniques and sensors with different operational principles can be used to monitor structural conditions [7,8]. Digital image correlation based tracking [9] can be used effectively in laboratory conditions to examine the overall deformation of the composites, but this method does not allow the monitoring of structural changes in the composite structure at its place of application and during operation (*in-situ*). After assembling and installing the composite part, one of the possibilities to monitor its conditions is to build a state monitoring sensor onto or into the composite structure and to predict the stress, deformation and the structural changes by the

signals of the sensors. By using the built-in or built-on sensors, it is possible to continuously monitor the internal deformations of the structure in-situ at its place of application of the composite without the need for its removal. A widely used method to measure the deformation of products is the application of strain gauges. The main element of the sensor is an electrically conductive folded wire, which is integrated onto an elastic insulator film. The strain gauge is fixed onto the monitored part, thus by the deformation of the insulator film, the resistance of the conductive layer will change, which is proportional to the strain.

To get information about the internal state of the material, and to protect the sensors, built-in sensors are preferred. Several papers focus on this topic, there are also some examples, where the structural health could be monitored without compromising the strength of the material, for example in the paper of Shen et al. [10], where carbon nanotube buckypapers were used as interleaves to monitor delamination.

### 1.2. FBG sensors for condition monitoring

The Fibre Bragg Grating (FBG) optical sensor is more and more

---

widely used for the monitoring of the condition of polymer composites, since this method provides precise deformation values with sufficient resolution and sensitivity. The optical fibre sensor can be integrated inside a polymer matrix composite, while the mechanical properties of the polymer composite structure do not decrease significantly, due to its small form factor. Thus the sensor can be used for monitoring the manufacturing process during production [11] and for structural health monitoring and failure analysis during application of the composite [12, 13]. The optical Bragg-grid is the series of thin, perpendicularly oriented strips of different refractive index than the core of the optical fibre placed in the core of the optical fibre [14,15]. When light is guided into the fibre, the gratings reflect a certain wavelength beam, while other wavelengths pass through without disturbance, depending on the refraction index and the distance of the Bragg-gratings. The distance of the gratings depends on the deformation and temperature. If this changes, other wavelength light will be reflected. The change in the distance of the gratings can be calculated by measuring the power depending on the wavelength of the reflected light, thus the wavelength lag [16]. Deformation is a result of external forces and thermal expansion. In the case of non-isothermal conditions, temperature compensation can be applied to calculate both strain components. Many authors have investigated the usability of FBG sensors for structural health monitoring (SHM) [17] to investigate damage from fatigue [18,19] or deformation induced by fatigue tests [20,21] but the sensors were only fixed on the composites surface, not integrated into the components. The applicability of FBG sensors to monitor the conditions of fatigue tested natural fibre reinforced polymer composites has not been investigated yet.

### 1.3. Fatigue behaviour of natural fibre composites

Natural fibres as bio-based reinforcing materials are gaining more and more attention as the importance of using renewable materials in structural parts is growing. While in the past decades their application was mostly limited to low load, non-critical parts, now automotive suppliers are increasingly using them in load-bearing structures [22], where their good, long-term mechanical performance is essential. Natural fibres have a much more complex structure and a tendency to show higher variances in mechanical properties [23,24] than synthetic fibres. Another drawback of natural fibre reinforced plastics is insufficient fibre/matrix adhesion, which can cause debonding between the fibre and the matrix over time [25]. For this reason, monitoring their condition [26] is even more crucial than in case of synthetic fibre reinforced composites. For their proper monitoring, some key aspects of their structural changes over time and their damage evolution have to be considered.

Baley [27] tested single flax fibres in static and fatigue tensile tests. They observed an increase in the Young's modulus of the fibre, which they explained with a strain-dependent reorganization of the microfibrils in the direction of the fibre axis during the test. The same trend is also present in other studies, in which fibre reinforced composites were tested in dynamic tensile-tensile test mode [28,29].

Mahboob et al. [30] investigated the damage evolution of flax fibre reinforced epoxy composites using iterative quasi-static load-unload sequences in the tensile and compression direction. The results show that composite damage during dynamic tests coincides with (i) a decreasing modulus and (ii) an accumulating permanent strain. They also found that the accumulation of permanent strain over the lifetime (i) shows continuous development for all tested loads, even when stiffness remains unchanged and (ii) is a significant parameter (besides stiffness) to track the microstructural damage evolution.

### 1.4. Aims of the study

We aim to demonstrate the possibility of integrating FBG sensors in natural fibre reinforced composites as embedded sensors for online

strain measurement by checking the precision and robustness of the embedded sensors under static loads. Our goal is to prove that embedded FBG sensors can be used for condition monitoring of the composite structures through the monitoring of damage progression during fatigue loading, focusing on specific, robust evaluation methods and using the characteristic properties provided by the embedded FBG sensors.

## 2. Materials and methods

### 2.1. Materials

The reinforcement fabric used for manufacturing the composite was a woven flax fibre textile (Biotex Flax 400 g/m$^2$ 2 × 2 Twill) supplied by Composites Evolution (Chesterfield, UK). The matrix system was a two-component DGEBA epoxy system for infusion processes (Epinal LR 80-A2.10) provided by bto-epoxy GmbH (Amstetten, Austria). With the given amine-based hardener (Epinal LH 80-B2.00), the resin system provides a pot life of 60 min at room temperature and cures within a recommended temperature range between 25 °C and 90 °C. The mixing weight ratio was 100:25 according to the producer's specification.

### 2.2. Composite production

The composite plates were produced by resin transfer moulding, with a mould having a square-shaped cavity of 270 mm × 270 mm and a height of 4 mm. The 6 layers of reinforcing material were impregnated in their full width with a line distributor. The mould carrier was a Langzauner LZT-OK-80-SO (Lambrechten, Austria) press. The resin was injected into the preheated mould (temperature: 50 °C) with a Walther V4422160012 pressure vessel with 2 bars of injection pressure. The injection was performed in a mould with open vents, which were closed when the resin appeared at both outlets. The pressure was kept on the resin for the whole curing process as post-pressure. Two FBG sensors were installed in every plate produced in the locations indicated in Fig. 1 between the fifth and sixth layer.

After around 9 h curing time at 50 °C the plates were removed from the mould. We used DSC tests to ensure that the composites were completely cured. The glass transition temperature of the epoxy system cured at 50 °C isothermally is 70 °C, measured by DSC and in accordance with the material data sheet. The specimens were cut to the desired dimensions with a diamond disc cutter. We measured the weight and geometry of the composites and their constituents. The fibre volume fraction of the composites was 37%.

### 2.3. Test methods

#### 2.3.1. Quasi-static four-point bending tests

The four-point bending tests were performed according to EN ISO 14125 with a Zwick Z250 computer-controlled tensile tester (Zwick, Ulm, Germany) equipped with a 20 kN load cell. Standard four-point bending fixtures were used with a 66 mm outer and a 22 mm inner span according to the standard specifications for method B. Test speed was 2 mm/min. During the test, we obtained the strain using four methods: we calculated it (using the elastic beam theory) from deflection data measured with the tensile tester, measured strain with a strain gauge, used digital image correlation (DIC), and used the embedded FBG sensors.

We applied MT-LIAS-06-3-350-5E strain gauges (MikroT Kft., Budapest, Hungary). The gauges were fixed to the surface of the specimens with Loctite 406 cyanoacrylate adhesive. The signal of the gauges was acquired with an HBM Spider 8 (Hottinger Baldwin Messtechnik, Darmstadt, Germany) DAQ unit. The data acquisition rate was 10 Hz.

Digital image correlation was measured with a Mercury BFLY 050 camera (Sobriety Sro., Kurim, Czech Republic) and the Mercury RT software. The data acquisition rate was 10 Hz.

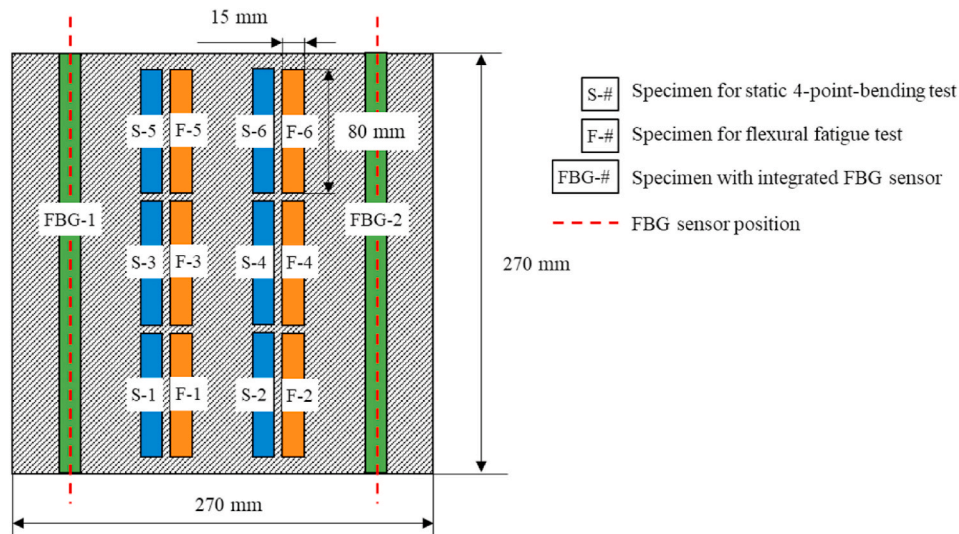Sylex FFA-01 sensors (Sylex, Bratislava, Slovakia) were used for FBG

**Fig. 1.** Layout of test specimens in the produced plates.

strain measurement. Data was acquired with a Sylex S-Line Scan 800 interrogator. The FBG interrogator has a depolarized light source, which helps minimize the effect of birefringence. The data acquisition rate was 1 Hz.

### 2.3.2. Fatigue tests

The four-point bending fatigue tests were performed with an Instron 8872 (Instron, Norwood, USA) computer-controlled servo-hydraulic test frame equipped with an Instron Fasttrack 8000 control and data acquisition unit and a 1000 N capacity Instron Dynacell load cell in load-controlled operation. Standard four-point bending fixtures were used with a 66 mm outer and a 22 mm inner span (identical to the quasi-static tests). The applied load waveform was sinusoid with a frequency of 10 Hz. We performed the quasi-static cycles between the fatigue regimes in the case of the FBG embedded specimens with conditions identical to those in the quasi-static tests. During the fatigue tests, we calculated strain from deflection measured with the tensile tester (based on the elastic beam theory), and measured strain directly with an FBG sensor.

### 2.3.3. Fatigue data evaluation

Based on the load data and recorded displacement in the fatigue test, we calculated the corresponding bending stress and strain values, respectively, using the given equations in the test standard method *DIN EN ISO 14125* for the 4-point-bending test mode. The flexural stress, $\sigma$, is defined as:

$$\sigma = \frac{FL}{bh^2} \tag{1}$$

where $F$ is the load, $L$ is support span width ($L = 66mm$), $b$ is specimen width, and $h$ is specimen height. The equation for flexural strain, $\varepsilon$, is as follows:

$$\varepsilon = \frac{4,7sh}{L^2} \tag{2}$$

where $s$ is the deflection of the midpoint of the specimen (calculated by multiplying the crosshead displacement by 1.15, according to the elastic string theory). We analysed the resulting stress-strain-hysteresis by evaluating three characteristic parameters (see Fig. 2). These modulus type characteristic properties are commonly used for damage progression monitoring, and we selected them as reference parameters. We evaluated the dynamic modulus, $E_{dyn}$, with the use of a straight line fit (least squares regression) to approximate the hysteresis slope based on the recorded data points. The slope of the straight line between the
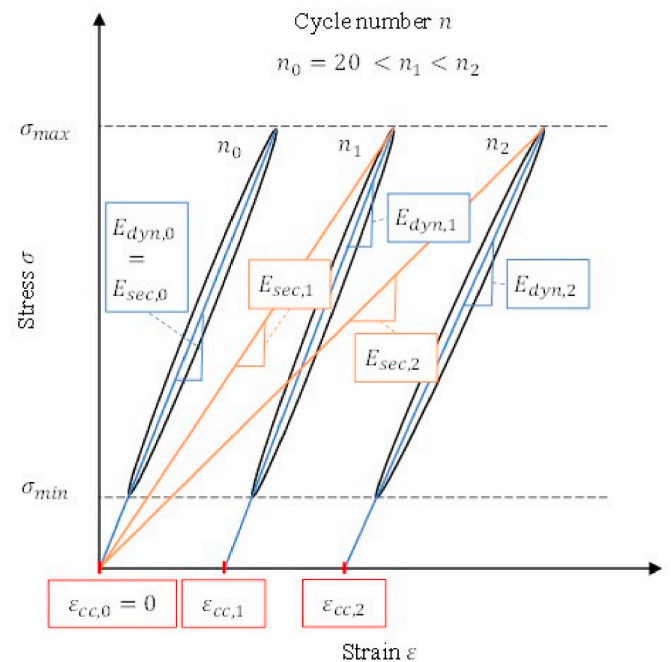


**Fig. 2.** Illustration of the development of hysteresis during a flexural fatigue test with the characteristic parameters: dynamic ($E_{dyn}$) and secant modulus ($E_{sec}$), cyclic-creep strain.($\varepsilon_{cc}$)

origin and the intersection point of the fitted hysteresis line and the maximum stress level, $\sigma_{max}$, is the secant modulus, $E_{sec}$. The extrapolated intersection point of the hysteresis line at a stress level of 0 *MPa* represents the cyclic creep strain, $\varepsilon_{cc}$, when the specimen is unloaded. The cyclic creep strain parameter was used to represent the permanent strain over the fatigue lifetime. Cyclic creep strain is a result of standard creep processes of the components of the composite. Standard creep processes are defined as time-dependent deformation under constant load, but in this context they also consider the impact of the accumulation of structural damage on permanent strain. Increasing defect density causes higher flexibility of the material, due to local fibre-matrix debonding, matrix cracks and fibre fractures, which result in an increasing plastic deformation. The calculation of the actual permanent strain does not take into account any viscoelastic effects present in real unloading cases.

Nevertheless, these approximated values show good correlation with the measurement data of the FBG sensor.

## 3. Results and discussion

### 3.1. Static validation

To prove the applicability of embedded FBG sensors for direct fine strain measurement and to get baseline strength data to determine load levels for the fatigue tests, we performed quasi-static four-point bending tests on the composite specimens. Besides the FBG sensors, we used three other strain measurement methods as reference. Fig. 3 shows the test setup.

We tested the composite specimens without FBG sensors until fracture occurred, to get information about the mechanical characteristics of the composite (Table 1). The tests indicated that the samples were of good quality, and the deviations were in the normal range. We defined the load levels in the consecutive fatigue tests based on the average values.

We examined possible errors caused by hysteresis and tested the repeatability and robustness of the tests with cyclic four-point bending tests on the composites with the embedded FBG sensors. We performed 4 static cycles on each specimen, up to 150 N, 200 N, 250 N and 300 N (altogether 16 tests on each specimen). The maximum force was limited to 300 N (approximately 80 MPa, 50% of $\sigma_{fM}$) so that it remained in the linear region, and the test was non-destructive. Fig. 5 shows characteristic curves obtained from the 150 N and 300 N cycles. Since the FBG sensor is located beneath the outer layer (there were a total of six layers), the measured strain has to be multiplied by 3/2 (the layers are assumed to be of equivalent thickness). This way, strain at the surface is obtained—the other methods measure the strain at the outer pulled surface (the strain gauges are attached to the surface and DIC also measures the strain at the surface of the specimen—see Fig. 4).

Fig. 5 shows that the correlation between the different measurement methods is very good and hysteresis is not present in any of the tests. The noise observed in case of the DIC curve is caused by the sensitivity of optical measurement to external effects. The strain gauges and the FBG provided very stable results, and in the case of this relatively low deformation level, calculation based on crosshead displacement was also accurate. The test results show that the FBG sensor can provide the strain directly with significant advantages. Compared to optical strain measurement, the signal is more stable and is not affected by lighting conditions. Compared to the strain gauge, the signal is not affected by electric fields.

### 3.2. Fatigue tests

After the quasi-static tests, we performed the main fatigue tests. In the load-controlled fatigue test, we used a sinusoidal load waveform

**Table 1**
Results of the quasi-static four-point bending tests (h – specimen thickness, b – specimen width, $E_f$ – flexural modulus of elasticity, $\sigma_{fM}$ – maximum flexural stress, $\varepsilon_M$ – strain at maximum flexural stress, $\sigma_{fB}$ – flexural stress at break, and $\varepsilon_B$ – strain at break).

| No. | h [mm] | b [mm] | $E_f$ [GPa] | $\sigma_{fM}$ [MPa] | $\varepsilon_{fM}$ [%] | $\sigma_{fB}$ [MPa] | $\varepsilon_B$ [%] |
|---|---|---|---|---|---|---|---|
| 1 | 3.92 | 14.82 | 9.61 | 141.48 | 2.00 | 141.48 | 2.00 |
| 2 | 3.93 | 15.01 | 10.10 | 150.10 | 2.06 | 150.10 | 2.06 |
| 3 | 3.91 | 14.96 | 9.94 | 146.83 | 2.17 | 146.83 | 2.17 |
| 4 | 3.91 | 14.93 | 10.24 | 151.63 | 2.15 | 151.63 | 2.15 |
| 5 | 3.91 | 15.10 | 10.11 | 149.63 | 2.07 | 149.63 | 2.07 |
| 6 | 3.92 | 14.95 | 10.06 | 150.55 | 2.20 | 150.55 | 2.20 |
| Average | | | 10.01 | 148.37 | 2.11 | 148.37 | 2.11 |
| Deviation | | | 0.22 | 3.74 | 0.08 | 3.74 | 0.08 |

between 400 N (approximately 75% of average maximum force) and 40 N (load factor, R = 10). The maximum load was selected so that the probable failure occurs in about 10,000 cycles, so damage accumulation can be observed.

### 3.2.1. Flexural fatigue test, hysteresis analysis

Fig. 6 shows how the relative dynamic modulus $E_{dyn,rel}$ of the tested specimen changed during the flexural fatigue test. $N/N_f$ is the fatigue life ratio, $N$ is the number of the current cycle and $N_f$ is the total cycle number until failure. There is a reproducible tendency in this test series: dynamic stiffness slightly increases and reaches a maximum between 60% and 80% of fatigue life. After 80%, the dynamic modulus decreases progressively until fatigue fracture. The values of $E_{dyn,rel}$ just before the final failure are below the initial stiffness, in the range between 0.75 and 0.95.

The increase in dynamic modulus, $E_{dyn}$ correlates well with the results from Asgarinia et al. [28,29]. In their studies, they characterized the stiffness of woven flax/epoxy composites with tension-tension fatigue tests. Their test results also show an increase in modulus in an early stage of fatigue life, with a subsequent reduction in stiffness at a continuous slow rate until failure. This stiffening effect can be explained on a micro-mechanical scale with the reorientation of cellulose fibrils in the flax fibre, which was shown by Baley [27]. He analysed the tensile stiffness increase of flax fibres and traced back the strain hardening effect to a change of micro-fibril angle with respect to the fibre axis during load. On mesoscopic level, the re-orientation of fibres inside the visco-elastic matrix can be another reason for the stiffening effect—this reorientation results in a more effective load distribution between the reinforcing fibres.

In general, the dynamic modulus is a parameter to characterize material damage during dynamic loading [31]. Considering this, it seems that the two mechanisms (1. stiffness decrease, due to material degradation and 2. stiffness increase, due to fibre re-orientation and load redistribution) compete with each other, leading to the development of
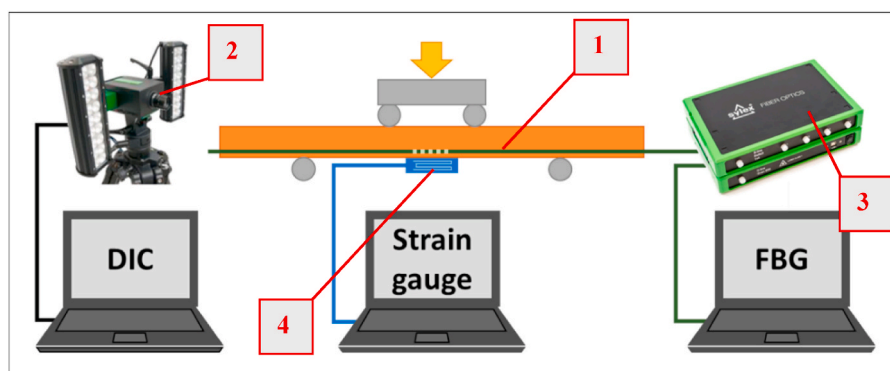


**Fig. 3.** The test setup of the quasi-static four-point bending tests (1 – specimen, 2 – camera for DIC, 3 – FBG interrogator, 4 –DAQ unit for strain gauge measurement).
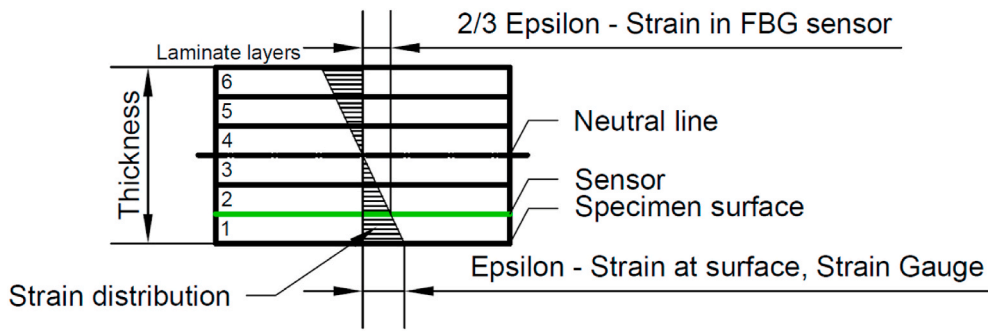
**Fig. 4.** Structure of the specimen, position of the embedded FBG sensor, calculation of surface strain from FBG sensor data.
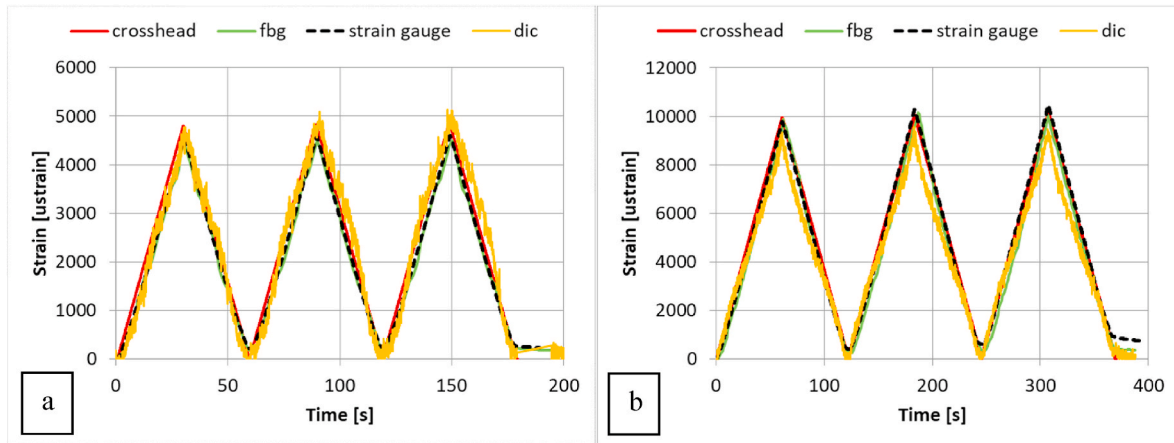


**Fig. 5.** Characteristic strain–time curves of the four-point bending tests obtained with the different strain measurement methods with corrected FBG strain data (a – cyclic test up to 150 N, b – cyclic test up to 300 N).
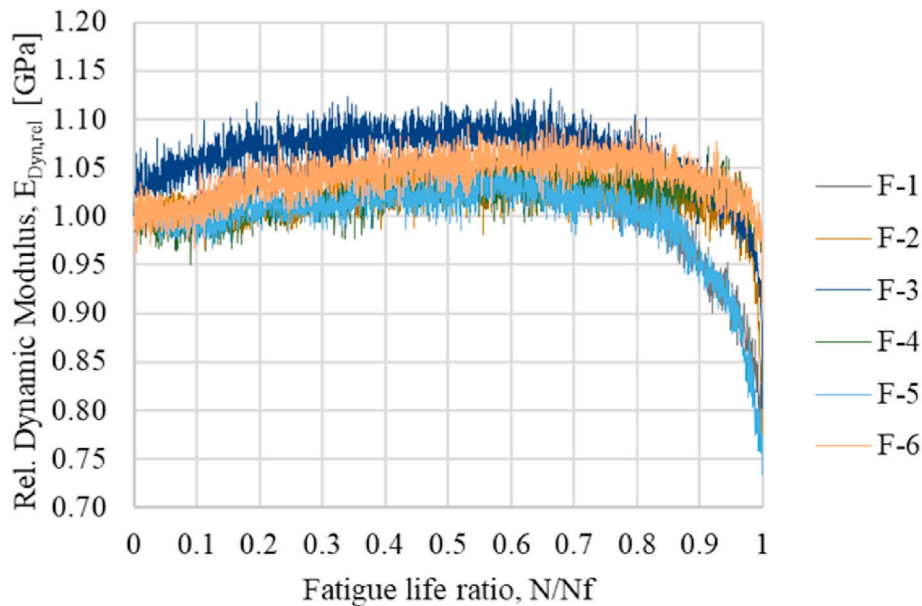


**Fig. 6.** Development of the relative Dynamic modulus over the fatigue life ratio of six representative specimens (F-1 – F-6).

$E_{dyn}$ that we observed.

The change of the secant modulus, as defined above, is influenced by the combination of the accumulated material damage as well as visco-elastic creep processes [31], which are in general mainly driven by the matrix material [32]. Fig. 7 shows the corresponding curves of the

relative secant modulus, $E_{sec,rel}$, as a function of fatigue life ratio. The tested specimens show a reproducible tendency that starts with a pronounced modulus reduction until around 20%–40% of fatigue life, followed by a section with a stable but reduced decrease rate. This linear behaviour stops between 60% and 80% of the fatigue life and ends in a
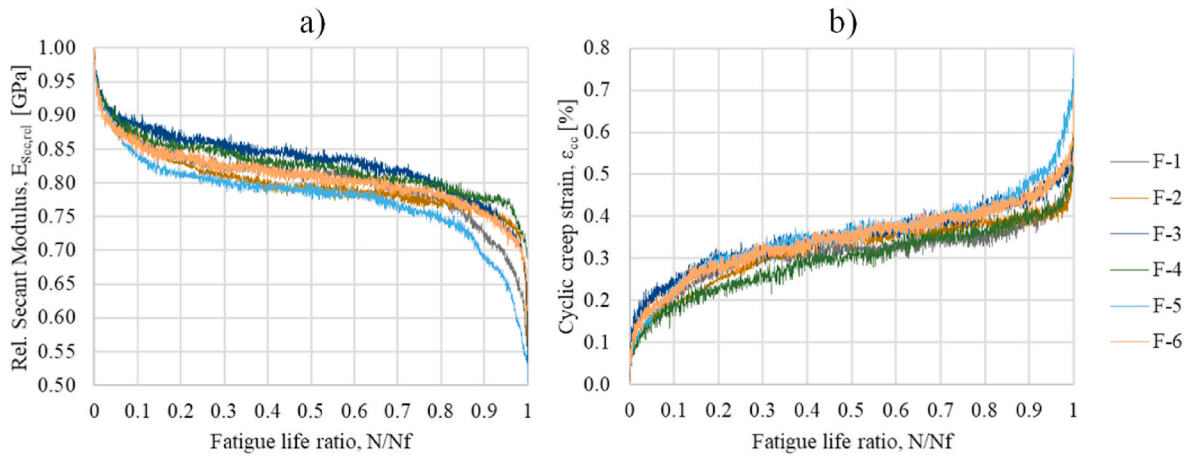
**Fig. 7.** a) Development of the relative Secant modulus as a function of fatigue life ratio, b) Development of cyclic creep strain as a function of the fatigue life ratio of six representative specimens (F-1 – F-6).

progressive decrease of $E_{sec}$ in the last stage of fatigue life until failure, similar to $E_{dyn}$.

Fig. 7a shows that the reduction of the secant modulus (decreasing slope of the approximated straight line) directly influences the extrapolated value for cyclic creep strain. Considering that the change of the secant modulus over the fatigue life is by definition more pronounced than the change of the dynamic modulus, the parameter for the calculated permanent deformation $\varepsilon_{cc}$ shows the same characteristics as the secant modulus. Fig. 7b shows the corresponding curves for the tested

specimen. The first phase is characterized by a pronounced increase in the evaluated cyclic creep strain until 20%–40% of the fatigue life is reached. Between 40% and 80% of fatigue life, the tendency of the stable increase of $\varepsilon_{cc}$ is observable and ends in a progressive increase until ultimate failure.

We used this degradation behaviour to prove that integrated FBG sensors can track the condition of the material in real time.
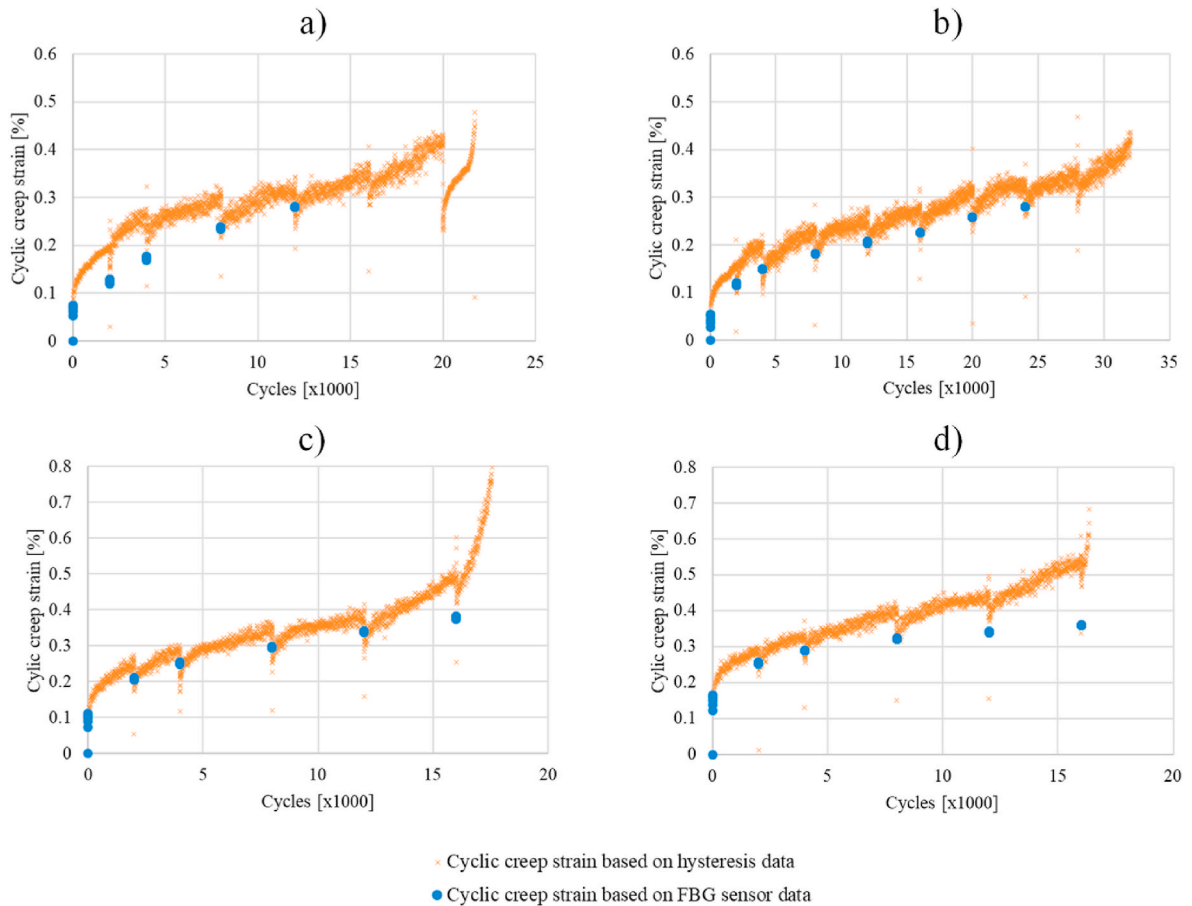


× Cyclic creep strain based on hysteresis data

● Cyclic creep strain based on FBG sensor data

**Fig. 8.** Comparison of the cyclic creep strain values obtained with the two different tests as a function of fatigue cycles for the four specimens (a–d) with integrated FBG sensors.

### 3.2.2. Evaluation of specimens with an integrated FBG sensor

After the evaluation of the fatigue test results of the composite specimens, we tested four specimens with integrated FBG sensors. To make the tests stable and reliable with the available maximum data acquisition rate of 1 Hz, we periodically slowed them down, and performed static cyclic FBG tests, similar to the tests presented before. These static tests were performed after 1000, 2000 and 4000 fatigue cycles, and afterwards after every 4000 fatigue cycles up to failure. For the evaluation of the condition of the material, we selected the cyclic creep strain value as the most reliable and reproducible property which can be directly measured with the integrated FBG sensors in unloaded condition. Fig. 8 shows the comparison of the cyclic creep strain values obtained from the FBG sensors, and cyclic creep strain calculated from hysteresis data.

The cyclic creep strain calculated from crosshead displacement is similar to the creep strain of the standard composite specimens. The only differences are the small steps after each static test, which we think are caused by the viscoelastic behaviour of the composites. During the static tests, the specimen can recover some of its delayed elastic strain component. Therefore, when we restarted the load-controlled fatigue test, the initial strain was lower after the static cyclic tests.

The tendency to get lower strain based on FBG data can be explained with the approximation method used for the calculation of the permanent strain based on the hysteresis data points. This approach neglects the viscoelastic behaviour in a real unloading process and therefore tends to overestimate the resulting $\varepsilon_{cc}$ value.

To investigate the possibility of using the evaluated cyclic creep strain to predict failure, we can use the maximum strain as the limiting fracture criterion. The static test results (Table 1) indicate that the fracture strain limit of the specimens is approximately 2.2%. The maximum cyclic strain during the fatigue tests was approximately 1.6%. During the fatigue cycles, total strain is the sum of cyclic creep strain and the amplitude of fatigue strain. In our case, the specimens failed after cyclic creep strain exceeded 0.4%, which results in a total strain above 2%. This correlates well with the average strain at break of the static tests performed without FBG sensors, keeping in mind that strain at break at higher load speeds are lower than those measured in static tests. We compared the data provided by the FBG sensors and data obtained with the standard method from crosshead displacement (modulus type characteristics) and found that while for strain, we can give a specific limit based on static or dynamic tests, determining the limiting values of modulus needs far more measurement and theoretical considerations.

Our results indicate that the embedded FBG sensors can be used effectively in fatigue-loaded structures for condition monitoring and the prediction of failure. The strain in the part can be monitored constantly or periodically. If it is checked periodically, the remaining deformation component can be followed, which gives information about the long-time creep effect of fatigue loading and the accumulation of damage in the part. When we know the limiting strain amplitudes during the normal operation of the part, operation can be stopped before the limiting strain is reached, therefore failure can be predicted and avoided. If an interrogator with suitable data acquisition frequency (which can be low, e.g. in the case of a cyclically pressurized and vented pressure vessel, or high in the case of a rotating or vibrating part) is available and integrated into the machine with the monitored composite part, testing can be continuous and on-line. Even automated fault-prevention protocols can be included which use the FBG signal as a limiting trigger.

Based on our results, we suggest the following improvements to enhance the robustness of the proposed condition monitoring method:

- The curves show loss of signal (missing points) in the first two tests. This can be caused by the damaged, fractured FBG sensor fibres, probably in the section between the interrogator and the grating. As an improvement, both ends of the sensor can be connected to the interrogator to ensure a redundant data acquisition. When the signal

is lost from one end, the other end can be automatically connected by an optical switch so that health monitoring is continuous.

- We assumed that the surrounding strain field is uniform and did not examine the quality of bonding between the sensor and the host matrix, which can slightly affect measurement results.
- We used sensors with only one set of gratings. There are sensors with multiple sets of gratings. The damage progress could be localized with the use of such sensors. When multiple sensors, or sensors with multiple gratings are used, the probability of getting information from the most severely damaged area is higher. The position of the fracture can also be estimated based on the highest measured strain. When the sensor has only one set of gratings, it has to be placed at the point with the highest probable load.

## 4. Conclusions

We demonstrated the applicability of FBG sensors for condition monitoring. In the first, static experiments, we compared FBG strain measurement results with optical and strain gauge strain measurement results. The test results indicate that the FBG sensor can show strain with significant advantages. Compared to optical strain measurement, the signal is more stable and not affected by lighting conditions and the signal is not affected by electric fields as in the case of strain gauges.

We performed four-point flexural tests to investigate the damage progression of the prepared composites. The test results indicated significant cyclic creep strain, so we selected it to monitor fatigue condition with the FBG sensors.

During the fatigue tests, the integrated FBG sensors provided information on the cyclic creep strain component. During the damage process, this component constantly increased and after a limit, where the strain under dynamic loading reaches the breaking strain of the static load, the specimen failed. The results indicate that the strain obtained with the integrated FBG sensors can be used to predict failure; they can also be used as a limiting value for failure prevention. We compared the data provided by the FBG sensors and data obtained with the standard method from crosshead displacement (modulus type characteristics) and found that while for strain, we can give a specific limit based on static or dynamic tests, determining the limiting values of modulus needs far more measurement and theoretical considerations.

### Declaration of competing interest

The authors declare that they have no known competing financial interests or personal relationships that could have appeared to influence the work reported in this paper.

### CRediT authorship contribution statement

**Gábor Szebényi:** Conceptualization, Methodology, Investigation, Visualization, Writing - original draft. **Yannick Blößl:** Conceptualization, Methodology, Investigation, Visualization, Writing - original draft. **Gergely Hegedüs:** Conceptualization, Methodology, Investigation, Visualization, Writing - original draft. **Tamás Tábi:** Writing - original draft. **Tibor Czigany:** Conceptualization, Methodology, Supervision, Writing - review & editing, Funding acquisition. **Ralf Schledjewski:** Conceptualization, Methodology, Supervision, Writing - review & editing, Funding acquisition.

### Acknowledgements

## References

[1] A. Alsaadi, J. Meredith, T. Swait, J.L. Curiel-Sosa, Y. Jia, S. Hayes, Structural health monitoring for woven fabric CFRP laminates, Compos. B Eng. 174 (2019), 107048.

[2] N. Forintos, T. Czigany, Multifunctional application of carbon fiber reinforced polymer composites: electrical properties of the reinforcing carbon fibers – a short review, Compos. B Eng. 162 (2019) 331–343.

[3] M.F. Ahmad Rasyid, M.S. Salim, H.M. Akil, J. Karger-Kocsis, Z.A.M. Ishak, Non-woven flax fibre reinforced acrylic based polyester composites: the effect of sodium silicate on mechanical, flammability and acoustic properties, Express Polym. Lett. 13 (6) (2019) 553–564.

[4] R. Zenasni, D.B. Maamar, Optimization of safety factor by genetic algorithm of circular notched carbon/epoxy laminate at low velocity impact, Period. Polytech. - Mech. Eng. 62 (3) (2018) 218–225.

[5] M.J. Mochane, T.C. Mokhena, T.H. Mokhothu, A. Mtibe, E.R. Sadiku, S.S. Ray, I. D. Ibrahim, O.O. Daramola, Recent progress on natural fiber hybrid composites for advanced applications: a review, Express Polym. Lett. 13 (2) (2019) 159–198.

[6] G. Romhány, L. Kovács, Derivation of ply specific stiffness parameters of fiber reinforced polymer laminates via inverse solution of classical laminate theory, Period. Polytech. - Mech. Eng. 62 (2) (2018) 158–164.

[7] G. Hegedűs, T. Sarkadi, T. Czigány, Multifunctional composite: reinforcing fibreglass bundle for deformation self-sensing, Compos. Sci. Technol. 180 (2019) 78–85.

[8] K.M. Tripathi, F. Vincent, M. Castro, J.F. Feller, Flax fibers – epoxy with embedded nanocomposite sensors to design lightweight smart bio-composites, Nanocomposites 2 (3) (2016) 125–134.

[9] G. Szebényi, V. Hliva, Detection of delamination in polymer composites by digital image correlation—experimental test, Polymers 11 (3) (2019).

[10] L. Shen, L. Liu, W. Wang, Y. Zhou, In situ self-sensing of delamination initiation and growth in multi-directional laminates using carbon nanotube interleaves, Compos. Sci. Technol. 167 (2018) 141–147.

[11] S. Konstantopoulos, E. Fauster, R. Schledjewski, Monitoring the production of FRP composites: a review of in-line sensing methods, Express Polym. Lett. 8 (11) (2014) 823–840.

[12] S. Minakuchi, N. Takeda, Recent advancement in optical fiber sensing for aerospace composite structures, Photon. Sens. 3 (4) (2013) 345–354.

[13] S.-W. Kim, E.-H. Kim, M.-S. Jeong, I. Lee, Damage evaluation and strain monitoring for composite cylinders using tin-coated FBG sensors under low-velocity impacts, Compos. B Eng. 74 (2015) 13–22.

[14] D. Kinet, P. Megret, K.W. Goossen, L. Qiu, D. Heider, C. Caucheteur, Fiber Bragg grating sensors toward structural health monitoring in composite materials: challenges and solutions, Sensors 14 (4) (2014) 7394–7419.

[15] N. Zeng, C.Z. Shi, C.C. Chan, M. Zhang, X.Y. Dong, Y.B. Liao, S.R. Lai, Enhancement of the measurement range of FBG sensors in a WDM network: a self-organizing network solution, Sensor Actuator Phys. 118 (2) (2005) 233–237.

[16] G. Luyckx, E. Voet, N. Lammens, J. Degrieck, Strain measurements of composite laminates with embedded fibre bragg gratings: criticism and opportunities for research, Sensors 11 (1) (2011) 384–408.

[17] W. Shen, R. Yan, L. Xu, G. Tang, X. Chen, Application study on FBG sensor applied to hull structural health monitoring, Optik 126 (17) (2015) 1499–1504.

[18] S. Yashiro, T. Okabe, Estimation of fatigue damage in holed composite laminates using an embedded FBG sensor, Compos. Appl. Sci. Manuf. 42 (12) (2011) 1962–1969.

[19] Q. Zhu, C. Xu, G. Yang, Experimental research on damage detecting in composite materials with FBG sensors under low frequency cycling, Int. J. Fatig. 101 (2017) 61–66.

[20] I. De Baere, G. Luyckx, E. Voet, W. Van Paepegem, J. Degrieck, On the feasibility of optical fibre sensors for strain monitoring in thermoplastic composites under fatigue loading conditions, Optic Laser. Eng. 47 (3) (2009) 403–411.

[21] W. Van Paepegem, I. De Baere, E. Lamkanfi, J. Degrieck, Monitoring quasi-static and cyclic fatigue damage in fibre-reinforced plastics by Poisson's ratio evolution, Int. J. Fatig. 32 (1) (2010) 184–196.

[22] N.A. Mohd Radzuan, D. Tholibon, A.B. Sulong, N. Muhamad, C.H.C. Haron, New processing technique for biodegradable kenaf composites: a simple alternative to commercial automotive parts, Compos. B Eng. 184 (2020), 107644.

[23] S. Amroune, B. Abderrezak, A. Dufresne, F. Scarpa, A. Imad, Investigation of the date palm fiber for green composites reinforcement: thermo-physical and mechanical properties of the fiber, J. Nat. Fibers 16 (2019).

[24] M.J. John, S. Thomas, Biofibres and biocomposites, Carbohydr. Polym. 71 (3) (2008) 343–364.

[25] J. George, M.S. Sreekala, S. Thomas, A review on interface modification and characterization of natural fiber reinforced plastic composites, Polym. Eng. Sci. 41 (9) (2001) 1471–1485.

[26] A. Hamdan, M.T.H. Sultan, F. Mustapha, 11 - structural health monitoring of biocomposites, fibre-reinforced composites, and hybrid composite, in: M. Jawaid, M. Thariq, N. Saba (Eds.), Structural Health Monitoring of Biocomposites, Fibre-Reinforced Composites and Hybrid Composites, Woodhead Publishing, 2019, pp. 227–242.

[27] C. Baley, Analysis of the flax fibres tensile behaviour and analysis of the tensile stiffness increase, Compos. Appl. Sci. Manuf. 33 (7) (2002) 939–948.

[28] D.U. Shah, Damage in biocomposites: stiffness evolution of aligned plant fibre composites during monotonic and cyclic fatigue loading, Compos. Appl. Sci. Manuf. 83 (2016) 160–168.

[29] S. Asgarinia, C. Viriyasuthee, S. Phillips, M. Dubé, J. Baets, A.W. Vuure, I. Verpoest, L. Lessard, Tension-tension fatigue behaviour of woven flax/epoxy composites, J. Reinforc. Plast. Compos. 34 (2015).

[30] Z. Mahboob, I. El Sawi, R. Zdero, Z. Fawaz, H. Bougherara, Tensile and compressive damaged response in Flax fibre reinforced epoxy composites, Compos. Appl. Sci. Manuf. 92 (2017) 118–133.

[31] G. Pinter, E. Ladstätter, W. Billinger, R.W. Lang, Characterisation of the tensile fatigue behaviour of RTM-laminates by isocyclic stress–strain-diagrams, Int. J. Fatig. 28 (10) (2006) 1277–1283.

[32] M. Elmessiry, Natural Fiber Textile Composite Engineering, 2016.